



Model calibration and validation for OFMSW and sewage sludge co-digestion reactors

G. Esposito^a, L. Frunzo^b, A. Panico^{c,*}, F. Pirozzi^c

^a Department of Mechanics, Structures and Environmental Engineering, University of Cassino, via Di Biasio 43, 03043 Cassino (FR), Italy

^b Department of Mathematics and Applications Renato Caccioppoli, University of Naples Federico II, via Cintia, Monte S. Angelo, I-80126 Naples, Italy

^c Department of Hydraulic, Geotechnical and Environmental Engineering, University of Naples Federico II, via Claudio 21, 80125 Naples, Italy

ARTICLE INFO

Article history:

Received 27 December 2010

Accepted 22 July 2011

Available online 17 August 2011

Keywords:

Anaerobic
Co-digestion
Hydrolysis
Mathematical modeling
Calibration
Validation

ABSTRACT

A mathematical model has recently been proposed by the authors to simulate the biochemical processes that prevail in a co-digestion reactor fed with sewage sludge and the organic fraction of municipal solid waste. This model is based on the Anaerobic Digestion Model no. 1 of the International Water Association, which has been extended to include the co-digestion processes, using surface-based kinetics to model the organic waste disintegration and conversion to carbohydrates, proteins and lipids. When organic waste solids are present in the reactor influent, the disintegration process is the rate-limiting step of the overall co-digestion process. The main advantage of the proposed modeling approach is that the kinetic constant of such a process does not depend on the waste particle size distribution (PSD) and rather depends only on the nature and composition of the waste particles. The model calibration aimed to assess the kinetic constant of the disintegration process can therefore be conducted using organic waste samples of any PSD, and the resulting value will be suitable for all the organic wastes of the same nature as the investigated samples, independently of their PSD. This assumption was proven in this study by biomethane potential experiments that were conducted on organic waste samples with different particle sizes. The results of these experiments were used to calibrate and validate the mathematical model, resulting in a good agreement between the simulated and observed data for any investigated particle size of the solid waste. This study confirms the strength of the proposed model and calibration procedure, which can thus be used to assess the treatment efficiency and predict the methane production of full-scale digesters.

© 2011 Elsevier Ltd. All rights reserved.

1. Introduction

Mathematical modeling of the anaerobic digestion process has been performed extensively during the last several decades. The first models that were proposed (Andrews, 1969, 1971; Lawrence, 1971; Andrews and Graef, 1971) are simple kinetic models that describe only the rate-limiting step of the biological process, i.e., the slowest step that limits the rate of the overall process. The limiting step of the anaerobic digestion process cannot be unequivocally defined, as the limiting step depends on the digester operating conditions (Castillo Monroy et al., 2006) and influent characteristics (Speece, 1983; Fricke et al., 2007). Acetogenesis (Hill, 1982; Bryers, 1985; Mosey, 1983; Costello et al., 1991a,b; Siegrist et al., 1993) and methanogenesis (Graef and Andrews, 1974; Hill and Barth, 1977; Kleinstreuer and Poweigha, 1982; Moletta et al., 1986; Smith et al., 1988), as well as hydrolysis (Pavlostathis

and Gossett, 1986; Vavilin et al., 2001) and disintegration (ADM1, Batstone et al., 2002; Esposito et al., 2008, 2009), can constitute the rate-determining steps.

Further models were developed to simulate the biochemical processes of the anaerobic digestion without preliminarily fixing the limiting step of the overall process (Vavilin et al., 1994; Angelidaki et al., 1999).

In 2002, the International Water Association (IWA) Task Group for Mathematical Modeling of Anaerobic Digestion Processes developed a comprehensive mathematical model known as Anaerobic Digestion Model no. 1 (ADM1, Batstone et al., 2002), which was based on experience acquired over the previous years in modeling and simulating the anaerobic digestion process.

This model, however, neglects some processes that are involved in the anaerobic digestion such as sulfate reduction, acetate oxidation, homoacetogenesis, solids precipitation and inhibition due to sulfide, nitrate, long chain fatty acids (LCFAs), and a weak acid and base (Batstone et al., 2002; Fuentes et al., 2008). Some of these previously discussed aspects have been subsequently studied and modeled. Two ADM1 upgrades were published in 2003 concerning the sulfate reduction (Fedorovich et al., 2003) and CaCO₃ precipitation

* Corresponding author. Tel.: +39 081 7683434; fax: +39 081 5938344.

E-mail addresses: giovanni.esposito@unicas.it (G. Esposito), luigi.frunzo@unina.it (L. Frunzo), anpanico@unina.it (A. Panico), francesco.pirozzi@unina.it (F. Pirozzi).

(Batstone and Keller, 2003). A further upgrade that was published in 2005 aimed to remove the ADM1 discrepancies in both carbon and nitrogen balances (Blumensaat and Keller, 2005).

A mathematical model was recently proposed by the authors (Esposito et al., 2008) to extend the ADM1 to simulate the anaerobic digestion of solid organic wastes. This model is intended to assess the performance of a sewage sludge and organic fraction of a municipal solid waste (OFMSW) co-digestion system regarding the chemical oxygen demand (COD) removal and methane production potential, including the simulation of the organic solid particle disintegration and the effect of LCFA production on pH. The model can assess the effect of the OFMSW particle size on the methane production rate. The application of the model showed that the presence of OFMSW particles makes the disintegration process, i.e., the decrease in size of the organic particles, the rate-limiting step for methane production (Hills and Nakano, 1984; Sharma et al., 1988; Esposito et al., 2008). This model can be used to assess the maximum organic loading rate (OLR) that an anaerobic digester can accept when fed with the OFMSW, predicting the pH drop and thus the digester failure as determined by the OLR excess.

The innovative aspect of this model is the kinetic expression that is used to model the conversion of the waste organic particles to carbohydrates, proteins and lipids (Esposito et al., 2008), i.e., the so-called disintegration process (Batstone and Keller, 2003). This model still applies first-order kinetics as used in most mathematical models available in the literature (Pavlostathis and Gossett, 1986; Vavilin et al., 1996; Batstone and Keller, 2003), but the kinetic constant is given as the product of two different terms with different physical meanings. The first term is the specific rate of the surface-based disintegration process (K_{sbk}) and depends only on the nature of the complex organic substrate. The second term is the overall surface area of the complex organic particles to be disintegrated per unit mass (a^*) and depends on the particle size distribution (PSD) of the solid substrate. If this model is compared with standard first-order kinetics where the disintegration kinetic constant depends on both the nature and PSD of the substrate, the main advantage of the model proposed by the authors is that K_{sbk} depends only on the organic substrate composition as the PSD is taken into account by the coefficient a^* . The K_{sbk} can thus be determined by experimental tests conducted on the material of any PSD.

In this study, biomethane potential (BMP) experiments were conducted on synthetic organic waste substrates with different PSDs to verify this assumption. The same experiments were used to set up a proper procedure to calibrate and validate the model, which is necessary for a suitable application of such a model to predict the performance of full scale digesters fed with sewage sludge and OFMSW.

2. Materials and methods

2.1. Experimental design

Biomethane potential (BMP) experiments were performed using synthetic organic waste substrates with known concentrations of carbohydrates, proteins and lipids. The choice of the substrates was determined by the need for the knowledge of carbohydrates, proteins and lipids in the digester influent, which are not easy to measure in OFMSW samples. Cumulative methane production from three different mixtures of synthetic organic waste and anaerobic sludge was investigated. Each mixture had the same composition expressed in terms of carbohydrates, lipids and proteins, but different particle sizes (Tables 1 and 2). In addition to the tests conducted in triplicate with the three solid organic mixtures, a further test was conducted using only anaerobic sludge as the organic substrate to estimate the volume of methane

Table 1

Composition of the organic mixtures in terms of the ratio between organic matter and anaerobic sludge, solid particle size and percentage of carbohydrates, lipids and proteins on a dry basis.

Test	($\frac{VS \text{ organic matter}}{VS \text{ anaerobic sludge}}$)	Initial radius [mm]	Carbohydrates [%]	Lipids [%]	Proteins [%]
A	1	0.5	70	12	18

Table 2

Mass composition of the organic mixtures (on a wet basis).

Test	Hard wheat pasta [g]	Cow cheese [g]	Anaerobic sludge [g]	Na ₂ CO ₃ [g]
A	15.0	4.4	150.0	0.20
B	15.0	4.2	173.0	0.20
C	15.0	4.4	150.0	0.20
D	–	–	–	0.10

resulting from the fermentation of the organics contained in the anaerobic sludge. Ten tests were performed.

2.2. Digester setup and operation

Anaerobic digestion was performed on a small scale under controlled and reproducible conditions in a 1000 mL glass bottle GL 45 (Schott Duran, Germany). Tap water was added to the mixture of the organic matter and anaerobic sludge up to a 500 mL total volume. Small amounts of Na₂CO₃ powder, ranging from 0.10 to 0.40 g, were also added to prevent a critical drop in the pH. Each bottle was sealed with a 5 mm silicone disc that was held tightly to the bottle head by a plastic screw cap punched in the middle (Schott Duran, Germany). All digesters were shaken for 30 min at 80 rpm by KL-2 (Edmund Bühler, Germany) bottle shakers and were immersed up to half of their height in hot water kept at a

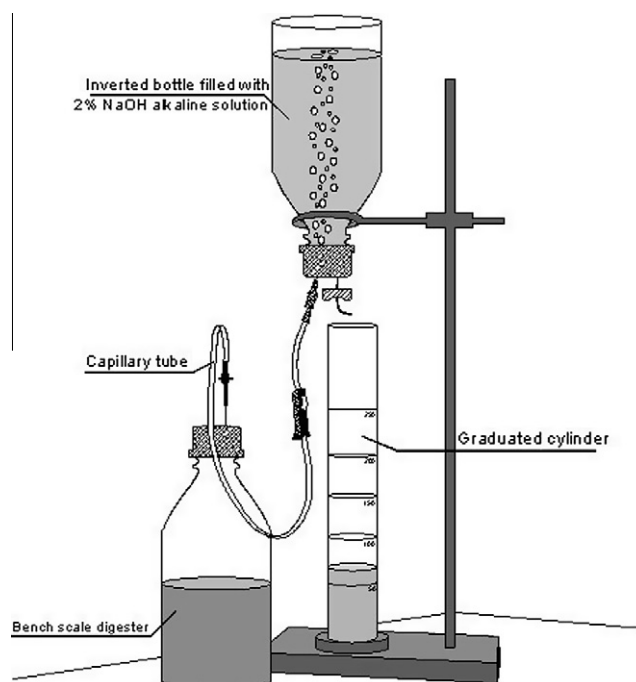


Fig. 1. Experimental equipment used to measure the daily methane production.

constant temperature of 308.15 K by 200 W A-763 submersible heaters (Hagen, Germany). Once a day, each digester was connected by a capillary tube to an inverted 1000 mL glass bottle containing an alkaline solution (2% NaOH). The inverted 1000 mL glass bottle was sealed in the same way as the digesters. To enable gas transfer through the two connected bottles, the capillary tube was equipped on both ends with a needle sharp enough to pierce the silicone disc (Fig. 1).

2.3. Digester feed

Three different criteria were used to select the composition of the synthetic organic waste used for biomethanation tests: (i) the ratio between anaerobic sludge and synthetic organic waste expressed in terms of Volatile Solids (VS) content; (ii) the synthetic organic waste particle size; (iii) the synthetic organic waste in terms of the content of carbohydrates, lipids and proteins. The three solid organic mixtures described in Tables 1 and 2 were made up using three types of pasta with different sizes, i.e., radius of 0.5 mm (*Tempestina* by pasta factory Rummo, Italy), 1.5 mm (*Spaghetti alla chitarra* by pasta factory Garofalo, Italy) and 2.5 mm (*Fregola* by pasta factory Quisardegna, Italy), and cow cheese (*Provolone dolce* by Soresina creamery, Italy), which was properly ground and sieved to achieve the same size as the pasta samples. Granular anaerobic sludge taken from an Upflow Anaerobic Sludge Blanket (UASB) reactor treating the wastewater produced by a potato processing factory was added to the three solid organic mixtures to reach a ratio between the VS contents of the anaerobic sludge and the synthetic solid waste equal to 1 (Tables 1 and 2).

2.4. Analytical measurements

2.4.1. Sludge and synthetic solid waste characterization

The weight, Total Solids (TS) and Volatile Solids (VS) concentration of the granular anaerobic sludge as well as the dry matter, moist organic matter and ash content of pasta, cheese and dewatered sludge were determined according to Standard Methods (APHA/AWWA/WEF, 1998). The composition of both pasta and cheese, in terms of carbohydrates, proteins and lipids, was taken from the respective packaging labels and was experimentally verified according to the procedures described in the Handbook of Food Analysis (Nollet, 2004).

2.4.2. Methane production

Daily methane production was monitored using an inverted 1000 mL glass bottle filled with a 2% NaOH solution and connected to the digester by a capillary tube (Fig. 1). The volume of alkaline solution displaced from the 1000-mL bottle, which was collected and measured using a graduated cylinder, was assumed to be equivalent to the volume of the daily methane production. The CO₂ contained in the biogas did not affect the volumetric methane measurements as the CO₂ was dissolved in the alkaline solution.

2.4.3. pH and temperature monitoring

Temperature and pH of all mixtures investigated were monitored for at least once a day with a TFK 325 thermometer (WTW, Germany) and a pH meter (Carlo Erba, Italy), respectively.

2.5. Mathematical modeling

The proposed mathematical model, which is described in detail by the equations in Appendices A and B, is based on the ADM1 approach but is modified to consider the features of a co-digestion system. The differential mass balance equations and the process kinetics and stoichiometry are modeled according to the ADM1,

and the same biochemical conversion processes (i.e., disintegration, hydrolysis, acidogenesis, acetogenesis and methanogenesis) are considered. However, the model can consider two different influent substrates (i.e., sewage sludge and OFMSW), which are modeled with different disintegration kinetics. First-order kinetics is used to model the sewage sludge disintegration according to the ADM1, and a surface-based kinetic expression (Sanders et al., 2000; Esposito et al., 2008) is used to simulate the OFMSW disintegration process, an essential step when the substrate to be disintegrated is as highly complex as the OFMSW.

This expression (Eq. (1)) considers the dependence of the OFMSW disintegration rate on the surface area (i.e., on the PSD) of the solid waste to be disintegrated. However, the surface-based kinetic expression proposed by Sanders et al. (2000) cannot be used in its original form (Eq. (1)) as the model structure needs the substrates to be expressed in terms of concentrations while Eq. (1) includes the organic particles in terms of mass:

$$\frac{dM}{dt} = -K_{sbk}A \quad (1)$$

where M = complex organic substrate mass [M]; K_{sbk} = disintegration kinetic constant [$M L^{-2} T^{-1}$]; A = disintegration surface area [L^2].

Eq. (1) has therefore been reformulated in terms of concentrations (Eq. (4)) by including the following two parameters, a and a^* , which characterize the disintegration process:

$$a = \frac{A}{V_{liq}} \quad (2)$$

$$a^* = \frac{A}{M} \quad (3)$$

$$\frac{dC}{dt} = -K_{sbk} \cdot a^* \cdot C \quad (4)$$

where C = concentration of the complex organic substrate in the digester [$M L^{-3}$]; V_{liq} = liquid working volume of the anaerobic digester [L^3].

Assuming that all the organic solid particles have the same spherical shape and initial size and that they are progressively and uniformly degraded, Eq. (3) can be rewritten as follows:

$$a^* = \frac{\sum_{i=1}^n A_i}{\sum_{i=1}^n M_i} = \frac{nA_i}{nM_i} = \frac{n4\pi R^2}{n\delta \frac{4}{3}\pi R^3} = \frac{3}{\delta R} \quad (5)$$

where A_i = disintegration surface area of the organic solid particle i [L^2]; M_i = mass of the organic solid particle i [M]; n = total number of organic solid particles [dimensionless]; δ = complex organic substrate density [$M L^{-3}$]; R = organic solid particles radius [L], assumed to be time dependent according to the following expression proposed by Sanders et al. (2000):

$$R = R_0 - K_{sbk} \frac{t}{\delta} \quad (6)$$

where R_0 = initial organic solid particle radius [L], specified as the initial condition for model application.

Eq. (4) therefore results in Eq. (7), which is used in the model:

$$\frac{dC}{dt} = -\left(\frac{3 \cdot K_{sbk}}{\delta}\right) \cdot \frac{C}{R} \quad (7)$$

Expressing C in Eq. (7) as the ratio between the mass of the organic solid particles and the digester volume results in the following quadratic dependence of the disintegration process rate on the particle radius:

$$\frac{dC}{dt} = -K_{sbk} \frac{n4\pi R^2(t)}{V_{liq}} \quad (8)$$

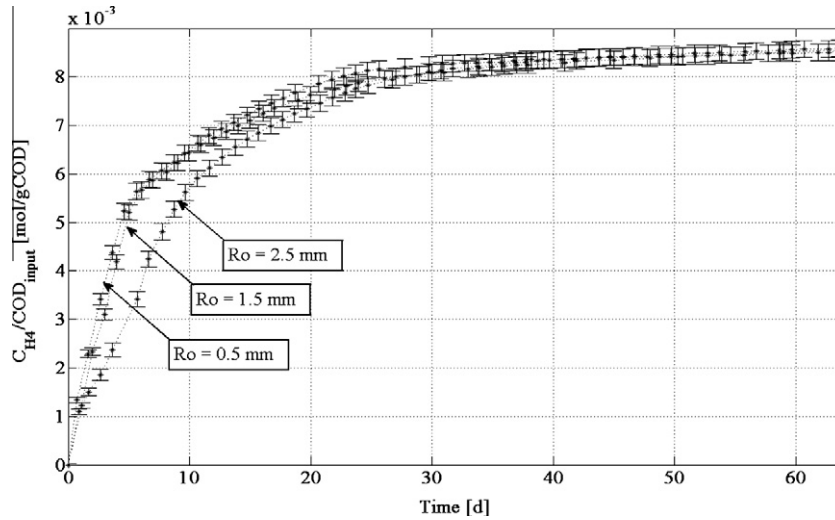


Fig. 2. Cumulative methane production obtained in the experimental tests A, B and C.

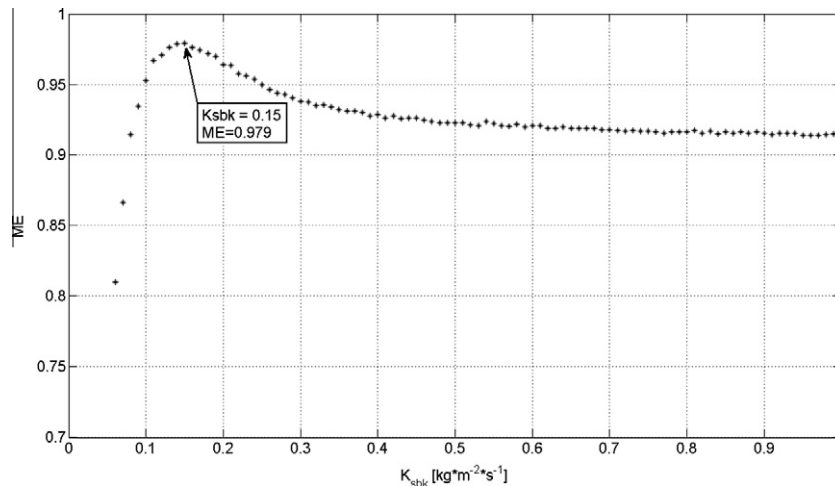


Fig. 3. Dependence of ME on K_{sbk} .

Because the radius of the organic solid particles varies according to a linear law (Eq. (6)), Eq. (8) implies that the concentration of the complex organic substrate decreases during the disintegration process according to a cubic law.

If this model is compared with the ADM1 first-order disintegration kinetics, the main advantage of this model is that K_{sbk} is the same for any OFMSW PSD and can thus be determined experimentally using OFMSW samples of any PSD. If a typical first-order kinetic expression is applied and organic waste samples are used to determine the kinetic constant experimentally, the latter can be used to simulate the anaerobic digestion of OFMSWs with only the same nature and PSD of the organic waste samples that are investigated.

Integration of the differential algebraic equations has been performed using a multi-step solution algorithm based on the numerical differentiation formulas in the software tool MATLAB®.

2.5.1. Model calibration and validation

Model calibration was used to estimate K_{sbk} ($M L^{-2} T^{-1}$), the kinetic constant of the surface-based disintegration process. Calibration was performed by comparing model results with experimental

measurements of methane production and adjusting the unknown parameter until the model results adequately fit the experimental observations.

Input, operational and output data from experiment A (Table 1) were used, and a specific procedure was developed.

The calibration procedure is structured in four steps as follows.

Step 1 determines a variation range for K_{sbk} . This range was set between 0 and 1 $kg\ COD\ m^{-2}\ d^{-1}$. This range was chosen because values of K_{sbk} smaller than 0 are physically not possible, and values greater than 1 are actually not significant because the model results are not sensitive to such values.

Step 2 generates as many different values of K_{sbk} as the estimation accuracy requires. This calculation was performed taking $n + 1$ constant step values of K_{sbk} , between the two bounds of the variation range, according to the following expression:

$$K_{sbk}^j = K_{sbk}^{j-1} + \Delta_{K_{sbk}}, \text{ with } j = 1 \dots n \quad (9)$$

where $K_{sbk}^0 = 0$ and $K_{sbk}^n = 1$ are the lower and upper bounds of the variation range, respectively, and $\Delta_{K_{sbk}}$ is the ratio between the width of the range and n .

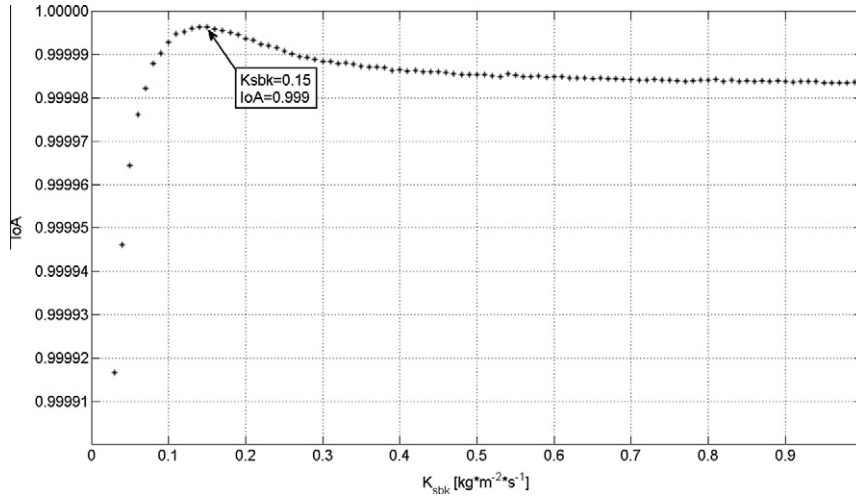


Fig. 4. Dependence of *IoA* on K_{sbk} .

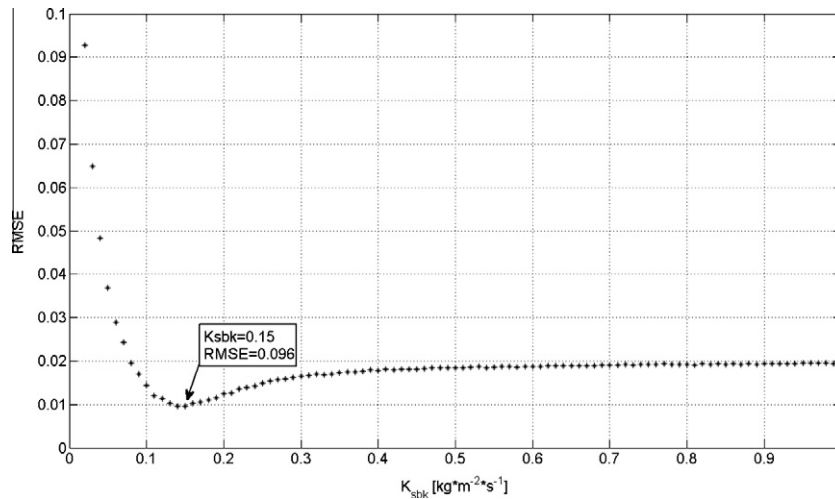


Fig. 5. Dependence of *RMSE* on K_{sbk} .

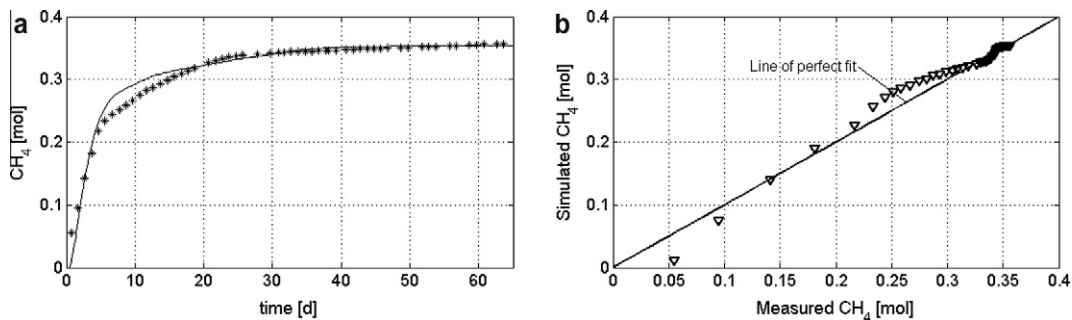


Fig. 6. Comparison of measured and simulated by proposed model cumulative methane production for experiments A: overlapping between measured and simulated data (a); comparison with the line of perfect fit (b).

To set the accuracy of the results at two significant digits, n was fixed to be equal to 100.

Step 3 was performed by plotting a simulated curve for each value of K_{sbk} from the development of step 2 and by comparing simulated results with observed data. A comparison was performed by applying three methods that are commonly used for the model calibration process (Janssen and Heuberger, 1993), the Modeling

Efficiency (*ME*) method, the Index of Agreement (*IoA*) method and the Root Mean Square Error (*RMSE*) method, calculating the three following parameters:

$$ME = 1 - \frac{\sum_{i=1}^K (y_i - y_i)^2}{\sum_{i=1}^K (y_i - y_M)^2} \quad (10)$$

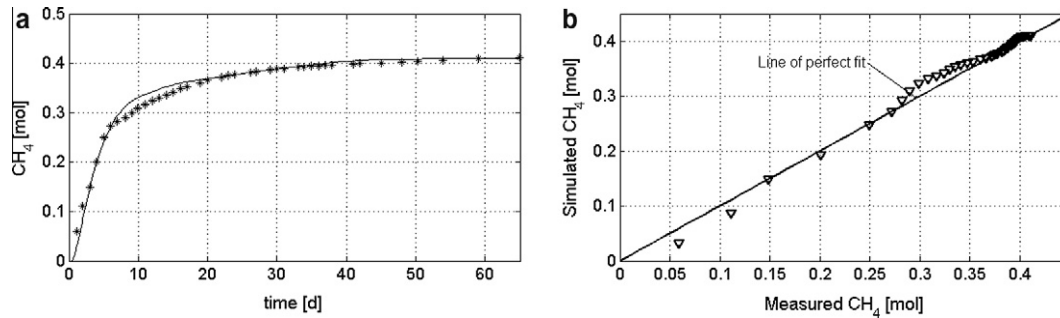


Fig. 7. Comparison of measured and simulated by proposed model cumulative methane production for experiments B: overlapping between measured and simulated data (a); comparison with the line of perfect fit (b).

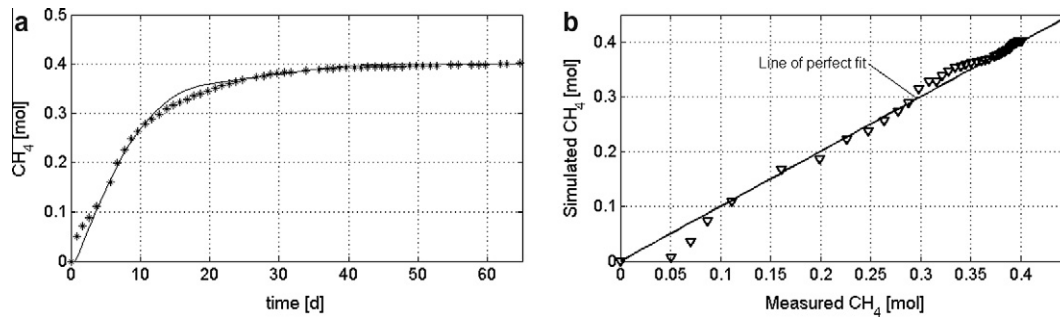


Fig. 8. Comparison of measured and simulated by proposed model cumulative methane production for experiments C: overlapping between measured and simulated data (a); comparison with the line of perfect fit (b).

$$IoA = 1 - \frac{\sum_{i=1}^K (y_i - y'_i)^2}{\sum_{i=1}^K (|y'_i - y_M| + |y_i - y_M|)^2} \quad (11)$$

$$RMSE = \sqrt{\frac{\sum_{i=1}^K (y_i - y'_i)^2}{K}} \quad (12)$$

where K = number of observed values; y_i = simulated value i ; y'_i = observed value i ; y_M = average of the simulated values.

Step 4 determines the value of K_{sbk} that best fits the observed data using the three different criteria. Step 4 is performed by plotting three series of points using Cartesian coordinates with K_{sbk} as the first coordinate and the corresponding values of ME , IoA and $RMSE$, calculated in step 3, as the second coordinate. The last operation of the calibration process is the determination of K_{sbk} that either maximizes ME as well as IoA or minimizes $RMSE$ for each series of plotted data.

After the calibration process was complete and the value of K_{sbk} was known, the model was validated to verify the agreement between the model results and the experimental measurements using the previously calibrated K_{sbk} value to simulate the digestion of synthetic organic waste (experiments B and C, Table 1) with a particle size different from the particle size of the synthetic organic waste (experiment A, Table 1) that was used for the calibration process. Model validation was performed by calculating ME , IoA and $RMSE$ for each set of simulated and observed data.

3. Results and discussion

The cumulative methane production data that were obtained from the experimental tests are reported in Fig. 2. This figure

shows that the gaps among the three curves resulting from tests A, B and C, respectively, are noticeable for the initial 20 days and then progressively tend to vanish. Within this initial period, the three curves are plainly distinguishable as clearly indicated by the error bars of the experimental points (Fig. 2). In particular, the differences are higher when the 2.5 mm curve is compared with the 0.5 or 1.5 mm curves. The differences among the three experimental curves are noticeable only during the initial 20 days, as the disintegration process of the solid particles occurs during this initial period. Once the solid particles have disintegrated, the anaerobic reactors continue to produce methane as long as all the organic matter is biodegraded, and the end points of the three curves coincide as each reactor was filled with the same amount of organic matter. The initial gap among the three curves is due to the effect of the solid particle size on the methane production, which cannot be properly modeled with the same first-order kinetic constant for the three experiments.

According to ADM1, a kinetic constant is required for each particle size. The main difference of the proposed model as compared with the ADM1 is that the disintegration rate constant K_{sbk} is invariant with the substrate particle size.

The model calibration performed in this paper resulted in setting the kinetic constant K_{sbk} to $0.15 \text{ kg m}^{-2} \text{ s}^{-1}$ when using values of the other kinetic and stoichiometric parameters as suggested by Batstone et al. (2002) for mesophilic solids.

This value of the kinetic constant K_{sbk} maximizes both ME and IoA and minimizes $RMSE$ (Figs. 3–5), making the gap between data simulated by model and experimental data used for the calibration process as small as possible. This K_{sbk} value fully meets the model calibration process requirements.

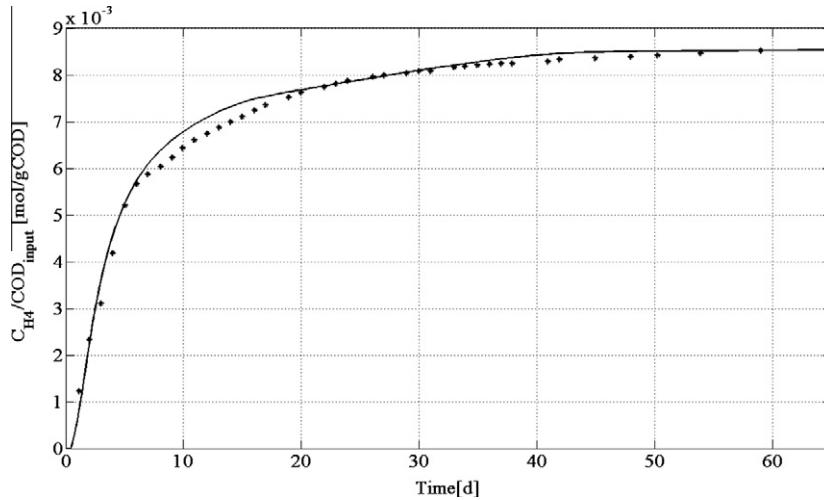


Fig. 9. Comparison of measured and simulated by ADM1 cumulative methane production for experiment B.

Table 3
Results of the model validation process.

Tests	R_0 [mm]	K_{sbk} [$\text{kg m}^{-2} \text{s}^{-1}$]	ME	IoA	RMSE
B	1.5	0.15	0.979	0.999	0.011
C	2.5	0.15	0.988	0.999	0.010

Table 4
Results of the ADM1 validation process.

Tests	R_0 [mm]	K_{dis} [$\text{kg m}^{-2} \text{s}^{-1}$]	ME	IoA	RMSE
B	1.5	0.406	0.985	0.999	0.010
C	2.5	0.406	0.909	0.996	0.031

All curves represented in Figs. 3–5 show a normal trend, characterized by a single monotone reversal located right in $K_{sbk} = 0.15 \text{ kg m}^{-2} \text{ s}^{-1}$. This reversal proves the existence of one and only one solution to the specific optimization problem that was used in this paper to calibrate the model.

A further interesting aspect that emerges by analyzing the previous three graphs concerns the sensitivity of *ME*, *IoA* and *RMSE* to K_{sbk} : the closer K_{sbk} is to $1 \text{ kg m}^{-2} \text{ s}^{-1}$, the smaller the variations of *ME*, *IoA* and *RMSE* are in response to variations in K_{sbk} . This last observation validates the hypothesis that the procedure used to calibrate the model is based on, to assume $1 \text{ kg m}^{-2} \text{ s}^{-1}$ as the upper bound of the K_{sbk} variation range.

The loss of sensitivity shown by the model toward values of K_{sbk} of $1 \text{ kg m}^{-2} \text{ s}^{-1}$ can be explained. K_{sbk} is a kinetic parameter used to describe the rate of a single process (i.e., disintegration) among the several processes involved in the anaerobic co-digestion of organic matter. The value of K_{sbk} can therefore affect the output of the model as long as it is small compared with the values of the other kinetic constants that are considered in the model (i.e., as long as disintegration is a limiting process). However, when the values of the different kinetic constants change, some processes that were not limiting become limiting and vice versa.

Fig. 6 shows the highest agreement between simulated and observed data for cumulative methane production achieved by the specific procedure that was used to calibrate the model. In Fig. 6a, the good overlap between the two series of data is shown,

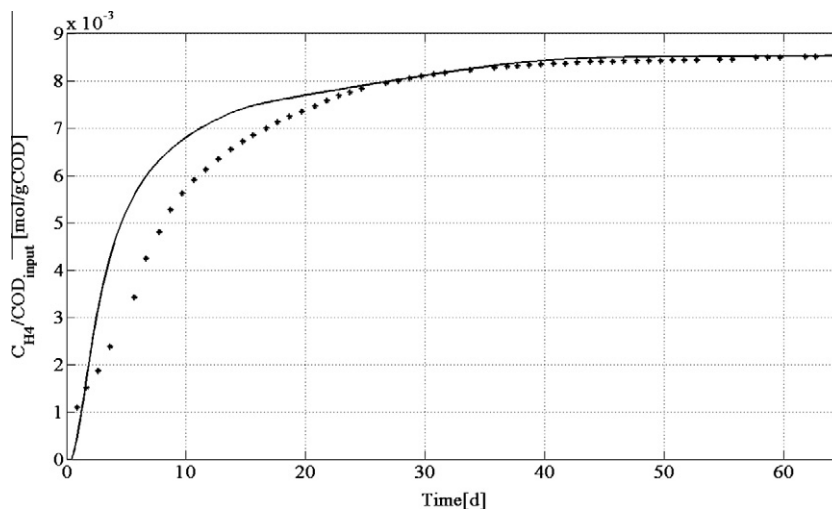


Fig. 10. Comparison of measured and simulated by ADM1 cumulative methane production for experiment C.

with a very small shift between the points with simulated and observed data as coordinates and the line of perfect fit reported in Fig. 6b.

After calibrating the model using the cumulative methane production results from experiment A, the calibrated K_{sbk} value (i.e., $0.15 \text{ kg m}^{-2} \text{ s}^{-1}$) was used to validate the model. Experiments B and C were used to validate the mathematical model, assessing the agreement between simulated and observed data for cumulative methane production with the parameters ME , IoA and $RMSE$. The results of the validation process are graphically described in Figs. 7 and 8 and are numerically reported in Table 3. The graphs indicate a very good agreement between the simulated and observed data; the agreement is confirmed by the values of the fitting parameters reported in Table 3. Only a few experimental points close to the origin of the axes are not fitted by the simulation results (Fig. 8a), showing a slight shifting from the line of perfect fit in Fig. 8b because of the readily biodegradable organic substrate present in the inoculum, which was not considered for the simulations.

The value assigned to K_{sbk} , as well as the modeling approach proposed in this paper, is fully validated by experiments B and C.

The same experimental data and the same calibration procedure applied to the proposed model were also used to calibrate and validate the ADM1 (Table 4 and Figs. 9 and 10) to assess the contribution of the proposed model as a potential upgrade for the ADM1. The calibration of the ADM1 resulted in a disintegration constant $K_{dis} = 0.406 \text{ s}^{-1}$, capable of maximizing both ME and IoA and minimizing $RMSE$ (Fig. 9). The validation process still resulted in acceptable values of ME , IoA and $RMSE$, but the values were not as good as the values obtained using the proposed model. Fig. 10 in particular shows an evident gap between the simulated and experimental data for the initial 25 days, i.e., when the particle size effect on the digestion process is more important. This gap confirms that the disintegration constant determined for a specific particle size cannot be properly used in ADM1 for a different particle size.

4. Conclusions

This paper focuses on the experimental determination of the surface-based kinetic constant K_{sbk} of the OFMSW disintegration process, the limiting step of the overall anaerobic co-digestion process when complex organic wastes such as OFMSW are fed to the reactor. The experiments demonstrated that K_{sbk} depends only on the nature and composition of the organic waste, while K_{sbk} is independent of the PSD of the OFMSW. The model calibration can therefore be performed on organic waste of any PSD and a PSD variation (e.g., if the OFMSW is pre-triturated) does not affect the calibrated K_{sbk} value.

Three different methods were applied to calibrate the model and all indicated a high modeling efficiency to corroborate the validity of the applied calibration procedure, which is confirmed by the optimal results of the validation process.

Acknowledgments

This research was supported by the Italian Ministry of the Research and the University in the framework of the National Research Project *Advanced Treatments for Organic Waste Reuse and Energy Recovery* funded in 2006 and the Research Project *Energy Saving with Valorisation of the Secondary Energy Sources as Distributed Energy Sources* funded in 2007 and by the Campania Region in the framework of the research project *Stabulum* funded in 2010.

Appendix A

Process	Component												Rate ρ_i [kg COD $\text{m}^{-3} \text{d}^{-1}$]
	1	2	3	4	5	6	7	8	9	10	11	12	
	S_{su}	S_{an}	S_{fa}	S_{va}	S_{bu}	S_{pro}	S_{ac}	S_{h2}	S_{ch4}	S_{ic}	S_{nv}	S_f	
1 Disintegration													$f_{dis} \cdot X_c$
2 Hydrolysis carbohydrates	1												$K_{sbk} \cdot \frac{C}{K} \cdot X_{ch}$
3 Hydrolysis proteins		1											$K_{hyd,pr} \cdot X_{pr}$
4 Hydrolysis lipids			1										$K_{hyd,li} \cdot X_{li}$
5 Uptake of sugars													$K_{msu} \cdot \frac{S_{su}}{K_{msu}} \cdot X_{su} \cdot I_1$
6 Uptake of amino acids													$K_{mae} \cdot \frac{S_{an}}{K_{mae}} \cdot X_{an} \cdot I_1$
7 Uptake of LCFA													$K_{mfa} \cdot \frac{S_{fa}}{K_{mfa}} \cdot X_{fa} \cdot I_2$
8 Uptake of valerate													$K_{mc4} \cdot \frac{S_{va}}{K_{mc4}} \cdot X_{c4} \cdot \frac{1}{1+S_{su}/S_{va}} \cdot I_2$
9 Uptake of butyrate													$K_{mc4} \cdot \frac{S_{bu}}{K_{mc4}} \cdot X_{c4} \cdot \frac{1}{1+S_{su}/S_{bu}} \cdot I_2$
10 Uptake of propionate													$K_{mpro} \cdot \frac{S_{pro}}{K_{mpro}} \cdot X_{pro} \cdot I_2$
11 Uptake of acetate													$K_{mac} \cdot \frac{S_{ac}}{K_{mac}} \cdot X_{ac} \cdot I_3$
12 Uptake of hydrogen													$K_{mh2} \cdot \frac{S_{h2}}{K_{mh2}} \cdot X_{h2} \cdot I_1$
13 Decay of X_{su}													$K_{decXsu} \cdot X_{su}$
14 Decay of X_{an}													$K_{decXan} \cdot X_{an}$
15 Decay of X_{fa}													$K_{decXfa} \cdot X_{fa}$
16 Decay of X_{c4}													$K_{decXc4} \cdot X_{c4}$
17 Decay of X_{pro}													$K_{decXpro} \cdot X_{pro}$
18 Decay of X_{ac}													$K_{decXac} \cdot X_{ac}$
19 Decay of X_{h2}													$K_{decXh2} \cdot X_{h2}$

Appendix B

Process	Component												Rate ρ_j [kg COD m ⁻³ d ⁻¹]
	13	14	15	16	17	18	19	20	21	22	23	24	
	S_{su}	S_{aa}	S_{fa}	S_{va}	S_{bu}	S_{pro}	S_{ac}	S_{h2}	S_{CH4}	S_{IC}	S_{IN}	S_I	
1 Disintegration	-1	$f_{Ch,Xc}$	$f_{Pr,Xc}$	$f_{Li,Xc}$									$f_{X_i,Xc}$
2 Hydrolysis carbohydrates		-1											$K_{s,bk} \cdot \frac{3}{\theta} \cdot \frac{C}{R}$
3 Hydrolysis proteins			-1										$K_{hyd, ch} \cdot X_{ch}$
4 Hydrolysis lipids				-1									$K_{hyd, pr} \cdot X_{pr}$
5 Uptake of sugars						Y_{su}							$K_{hyd, li} \cdot X_{li}$
6 Uptake of amino acids							Y_{aa}						$K_{m, su} \cdot \frac{S_{su}}{K_s + S_{su}} \cdot X_{su} \cdot I_1$
7 Uptake of LCFA								Y_{fa}					$K_{m, aa} \cdot \frac{S_{aa}}{K_s + S_{aa}} \cdot X_{aa} \cdot I_1$
8 Uptake of valerate									Y_{c4}				$K_{m, fa} \cdot \frac{S_{fa}}{K_s + S_{fa}} \cdot X_{fa} \cdot I_2$
9 Uptake of butyrate										Y_{c4}			$K_{m, c4} \cdot \frac{S_{c4}}{K_s + S_{c4}} \cdot X_{c4} \cdot \frac{1}{1 + S_{bu}/S_{su}} \cdot I_2$
10 Uptake of propionate											Y_{pro}		$K_{m, c4} \cdot \frac{S_{c4}}{K_s + S_{c4}} \cdot X_{c4} \cdot \frac{1}{1 + S_{va}/S_{su}} \cdot I_2$
11 Uptake of acetate											Y_{ac}		$K_{m, pro} \cdot \frac{S_{pro}}{K_s + S_{pro}} \cdot X_{pro} \cdot I_2$
12 Uptake of hydrogen												Y_{h2}	$K_{m, ac} \cdot \frac{S_{ac}}{K_s + S_{ac}} \cdot X_{ac} \cdot I_3$
13 Decay of X_{su}	1				-1								$K_{m, h2} \cdot \frac{S_{h2}}{K_s + S_{h2}} \cdot X_{h2} \cdot I_1$
14 Decay of X_{aa}	1					-1							$K_{dec, Xsu} \cdot X_{su}$
15 Decay of X_{fa}	1							-1					$K_{dec, Xaa} \cdot X_{aa}$
16 Decay of X_{c4}	1								-1				$K_{dec, Xfa} \cdot X_{fa}$
17 Decay of X_{pro}	1									-1			$K_{dec, Xc4} \cdot X_{c4}$
18 Decay of X_{ac}	1										-1		$K_{dec, Xpro} \cdot X_{pro}$
19 Decay of X_{h2}	1											-1	$K_{dec, Xac} \cdot X_{ac}$
													$K_{dec, Xh2} \cdot X_{h2}$

References

- Andrews, J.F., 1969. Dynamic model of the Anaerobic Digestion Model. J. Sanit. Eng. Div. Proc. Am. Soc. Civ. Eng. SA 1, 95–116.
- Andrews, J.F., 1971. Kinetic models of biological waste treatment processes. Biotechnol. Bioeng. Symp. 2, 5–33.
- Andrews, J.F., Graef, S.P., 1971. Dynamic modelling and simulation of the anaerobic digestion process. In: Pohland, F.G. (Ed.), Anaerobic Biological Treatment Processes, Advances in Chemistry, Series 105. American Chemical Society, Washington, DC (USA), pp. 126–162.
- Angelidaki, I., Ellegard, L., Ahring, B.K., 1999. A comprehensive model of anaerobic bioconversion of complex substrates to biogas. Biotechnol. Bioeng. 63, 363–372.
- APHA/AWWA/WEF, 1998. Standards Methods for the Examination of Water and Wastewater, 20th ed. United Book Press, Inc., Baltimore, Maryland (USA).
- Batstone, D.J., Keller, J., 2003. Industrial applications of the IWA Anaerobic Digestion Model no. 1 (ADM1). Water Sci. Technol. 47, 199–206.
- Batstone, D.J., Keller, J., Angelidaki, I., Kalyuzhnyi, S.V., Pavlostathis, S.V., Rozzi, A., Sanders, W.T.M., Siegrist, H., Vavilin, V.A., 2002. Anaerobic Digestion Model No. 1, Rep. No. 13. ed. IWA Publishing, London (UK).
- Blumensaat, F., Keller, J., 2005. Modelling of two-stage anaerobic digestion using the IWA Anaerobic Digestion Model no. 1 (ADM1). Water Res. 39, 171–183.
- Bryers, J.D., 1985. Structured modelling of the anaerobic digestion of biomass particulates. Biotechnol. Bioeng. 27, 638–649.
- Castillo Monroy, E.F., Cristancho, D.E., Arellano Abaunza, V., 2006. Study of the operational conditions for anaerobic digestion of urban solid wastes. Waste Manage. 26, 546–556.
- Costello, D.J., Greenfield, P.F., Lee, P.L., 1991a. Dynamic modelling of a single-stage high-rate anaerobic reactor – I. Model derivation. Water Res. 25, 847–858.
- Costello, D.J., Greenfield, P.F., Lee, P.L., 1991b. Dynamic modelling of a single-stage high-rate anaerobic reactor – II. Model verification. Water Res. 25, 859–871.
- Esposito, G., Frunzo, L., Panico, A., d'Antonio, G., 2008. Mathematical modelling of disintegration-limited co-digestion of OFMSW and sewage sludge. Water Sci. Technol. 58 (7), 1513–1519.
- Esposito, G., Frunzo, L., Panico, A., Pirozzi, F., 2009. Mathematical prediction of methane formation in an anaerobic co-digestion CSTR. In: Proceeding of the Fifth Dubrovnik Conference on Sustainable Development of Energy, Water and Environment System, Dubronik, 29th September–3rd October 2009, FP_320.
- Fedorovich, V., Lens, P., Kalyuzhnyi, S.V., 2003. Extension of Anaerobic Digestion Model no. 1 with process of sulphate reduction. Appl. Biochem. Biotechnol. 109, 33–45.
- Fricke, K., Santen, H., Wallmann, R., Hüttner, A., Dichtl, N., 2007. Operating problems in anaerobic digestion plants resulting from nitrogen in MSW. Waste Manage. 27, 30–43.
- Fuentes, M., Scenna, N.J., Aguirre, P.A., Mussati, M.C., 2008. Application of two Anaerobic Digestion Models to biofilm systems. Biochem. Eng. J. 38, 259–269.
- Graef, S.P., Andrews, J.F., 1974. Stability and control of anaerobic digestion. J. Water Pollut. Control Fed. 46, 667–682.
- Hill, D.T., 1982. A comprehensive dynamic model for animal waste methanogenesis. Trans. ASAE 25, 1374–1380.
- Hill, D.T., Barth, C.L., 1977. A dynamic model for simulation of animal waste digestion. J. Water Pollut. Control Fed. 10, 2129–2143.
- Hills, D.J., Nakano, K., 1984. Effects of particle size on anaerobic digestion of tomato solid wastes. Agric. Wastes 10, 285–295.
- Janssen, P.H.M., Heuberger, P.S.C., 1993. Calibration of process-oriented models. Ecol. Model. 83, 55–66.
- Kleinstreuer, C., Poweigha, T., 1982. Dynamic simulator for anaerobic digestion process. Biotechnol. Bioeng. 24, 1941–1951.
- Lawrence, A.W., 1971. Application of process kinetics to design of anaerobic processes. In: Pohland, F.G. (Ed.), Anaerobic Biological Treatment Processes, Advances in Chemistry, Series 105. American Chemical Society, Washington, DC (USA), pp. 163–189.
- Moletta, R., Verrier, D., Albagnac, G., 1986. Dynamic modelling of anaerobic digestion. Water Res. 20, 427–434.
- Mosey, F.E., 1983. Mathematical modelling of the anaerobic digestion process: regulatory mechanisms for the formation of short-chain volatile acids from glucose. Water Sci. Technol. 15, 209–232.
- Nollet, L.M.L. (Ed.), 2004. Handbook of Food Analysis, second ed., revised and expanded. Marcel Dekker, Inc., New York (USA).
- Pavlostathis, S.G., Gossett, J.M., 1986. A kinetic model for anaerobic digestion of biological sludge. Biotechnol. Bioeng. 28, 1519–1530.
- Sanders, W.T.M., Geerink, M., Zeeman, G., Lettinga, G., 2000. Anaerobic hydrolysis kinetics of particulate substrates. Water Sci. Technol. 41, 17–24.
- Sharma, S.K., Mishra, I.M., Sharma, M.P., Saini, J.S., 1988. Effect of particle size on biogas generation from biomass residues. Biomass 17, 251–263.
- Siegrist, H., Renggli, D., Gujer, W., 1993. Mathematical modelling of anaerobic mesophilic sewage sludge treatment. Water Sci. Technol. 27, 25–36.
- Smith, P.H., Bordeaux, F.M., Goto, M., Shiralipour, A., Wilke, A., Andrews, J.F., Ide, S., Barnett, M.W., 1988. Biological production of methane from biomass. In: Smith, W.H., Frank, J.R. (Eds.), Methane from Biomass. A Treatment Approach. Elsevier, London (U.K.), pp. 291–334.
- Speece, R.E., 1983. Anaerobic biotechnology for industrial wastewater treatment. Environ. Sci. Technol. 17 (9), 416–427.
- Vavilin, V.A., Vasiliev, V.B., Ponomarev, A.V., Rytov, S.V., 1994. Simulation model “methane” as a tool for effective biogas production during anaerobic conversion of complex organic matter. Bioresource Technol. 48, 1–8.
- Vavilin, V.A., Rytov, S.V., Lokshina, L.Ya., 1996. A description of hydrolysis kinetics in anaerobic degradation of particulate organic matter. Bioresource Technol. 56, 229–237.
- Vavilin, V.A., Rytov, S.V., Lokshina, L.Ya., Rintala, J.A., 2001. Simplified hydrolysis models for the optimal design of two stage anaerobic digestion. Water Res. 35 (17), 4247–4251.